EXTENDED REPORT

Topographical changes of biconvex objects during equatorial traction: an analogy for accommodation of the human lens

Ronald A Schachar, Deborah Kuchnir Fygenson

Br J Ophthalmol 2007;**91**:1698–1703. doi: 10.1136/bjo.2006.094888

See end of article for authors' affiliations

Correspondence to: Dr Ronald A Schachar, PO Box 601149, Dallas, Texas 75229, USA; ron@2ras.com

Accepted 13 June 2006
Published Online First 19 July 2006

Aim: To assess and compare the changes in shape of encapsulated biconvex structures undergoing equatorial traction with those changes reported in the human lens during accommodation.
Methods: Equatorial traction was applied to several different biconvex structures: air, water, and gel filled mylar and rubber balloons and spherical vesicles. In the vesicles, traction was applied externally, using optical tweezers, or from within, by the assembly of encapsulated microtubules. The shape changes were recorded photographically and the change in central radius of curvature of water filled mylar balloons was quantified.
Results: Whenever an outward equatorial force was applied to the long axis of *long oval* biconvex objects, where the minor to major axis ratio was $\leqslant 0.6$, the central surfaces steepened and the peripheral surfaces flattened. Similar changes in the shape of the lens have been reported during human in vivo accommodation.
Conclusions: All biconvex structures that have been studied demonstrate similar shape changes in response to equatorial traction. This effect is independent of capsular thickness. The consistent observation of this physical change in the configuration of biconvex structures in response to outward equatorial force suggests that this may be a universal response of biconvex structures, also applicable to the human lens undergoing accommodation.

The mechanism of accommodation has been studied for over 400 years.[1–16] Accommodation results from a change in the shape of the crystalline lens.[1] The lens is an encapsulated biconvex object. This change in shape of the lens occurs as a result of the force of ciliary muscle contraction transmitted circumferentially to the equatorial capsular edge of the lens by the zonules.

The widely accepted Helmholtz theory[2] states that during ciliary muscle contraction the tension on the zonules is reduced, allowing the lens to become rounder and to increase in central optical power. This theory was founded, in part, on an intuitive belief that the application of equatorial tension to the lens will flatten both its central and its peripheral surfaces.

As the lens is an encapsulated biconvex object, we tested this assumption by recording the cross sectional profiles of other encapsulated biconvex objects in response to equatorial tension.

METHODS

Balloons

Biconvex 9 inch mylar balloons with a wall thickness of 0.020 mm, and biconvex 8 inch rubber balloons, with wall thickness of 0.350 mm, were filled with either air, water, or gelatin. When filled, the balloons had a *long oval* profile,[17] with minor and major axes of ~175 mm and ~100 mm, respectively. The elastic moduli of rubber and mylar are 4 MPa and 3 GPa, respectively.

Each balloon was placed horizontally on an optical bench so that its equatorial plane was parallel to the bench. A circular ring light was centred above the balloon. The surface of the rubber balloon was made reflective by applying mineral oil. The changes in the reflection of the ring light from the surface of the balloon were videographed while equatorial traction was manually applied in one meridian or in two orthogonal meridians.

Radius of curvature measurement

A positional reference, a 6.35 mm diameter circular self-adhesive red paper dot was attached at the central pole of the upper surfaces of three water-filled mylar balloons. A Klein keratoscope that had been modified by removing its central convex lens was positioned above the balloon and centred at the positional reference. The distance between the positional reference and the keratometer was measured with an electronic digital caliper.

Two horizontally mounted, electronically controllable micrometers were attached to the equator of the balloon, 180° apart. The keratometric images associated with 20 outward micrometer steps of 0.5 mm, followed by 20 inward steps of 0.5 mm, were digitally photographed and measured in pixels. From the known diameter of the image of the paper reference dot, the diameter of the reflection of the second keratometric ring was determined in millimetres. The magnification, m, of the reflection of the second ring was calculated for each 0.5 mm tractional step. Using the object distance, s_o, which was the distance between the keratoscope and the pole of the balloon, the image distance, s_i, was calculated using the following formula[18]:

$$s_i = -s_o \times m$$

Then the central radius of curvature, r, was calculated from the mirror formula[18]:

$$r = \frac{-2}{1/s_i + 1/s_o}$$

Verification of the curvature measurement

Using the technique described above, the radii of six chrome alloy steel precision metric balls traceable to NIST were measured. Each ball incrementally increased in diameter in 1 mm steps from 25 mm to 30 mm, with a precision of ± 0.0025 mm. Each ball was measured in the 90° and 180° meridians five independent times.

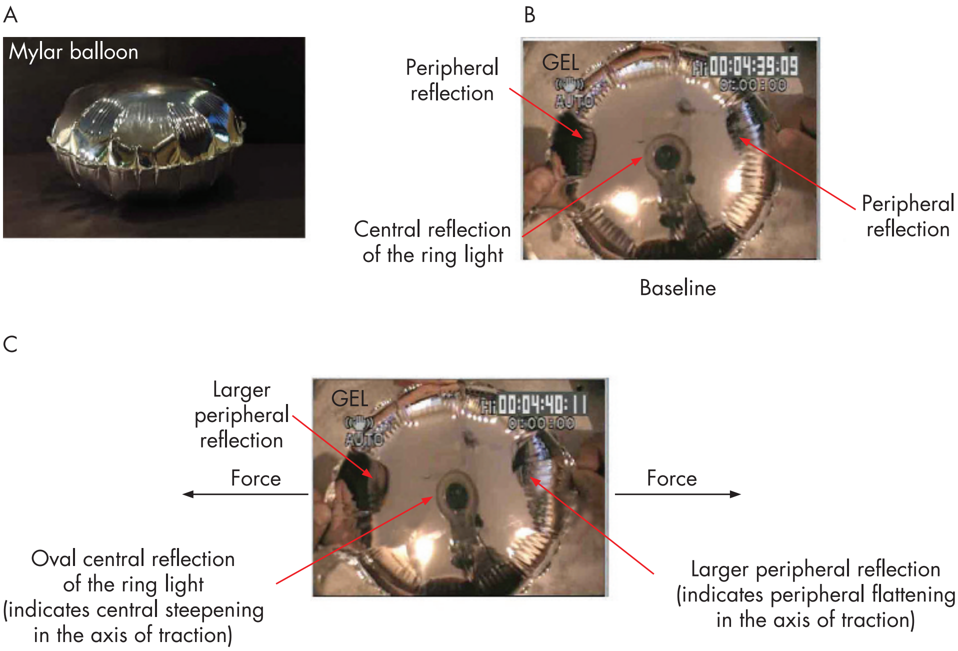

Figure 1 (A) Air filled Mylar balloon. (B) A gel filled Mylar balloon at baseline. (C) During equatorial traction in one meridian

Vesicles

An external force was applied to giant unilamellar vesicles (~10 µm diameter) in one meridian using a laser tweezers. A microscope stage was translated to bring the edge of a vesicle into the laser spot, and then translated slowly and horizontally away from the spot to apply the equatorial traction. The other end of the equator of the vesicle was pinned to the microscope slide. This ensured that the vesicle was only able to move in one plane and could not rotate.[19 20] In addition, an outward equatorial force was applied from within the vesicles in one meridian by the polymerisation of encapsulated microtubular fibres.[19 20] The vesicle profiles in response to the internal and external forces were videographed.

RESULTS

Balloons

Qualitative curvature change

Equatorial traction applied at one meridian or at four points spaced 90° apart resulted in central steepening and peripheral flatting of the surfaces of the mylar and rubber balloons, whether they were filled with air, water, or gelatin (figs 1 and 2).

Validation of curvature measurements

The mean difference between the measured radii and the actual radii of curvatures of the precision steel balls was 0.2 mm ±0.3 mm. Therefore, the accuracy of the measuring technique[21] for the radius of curvature of the balloons was better than 1.0 mm (fig 3).

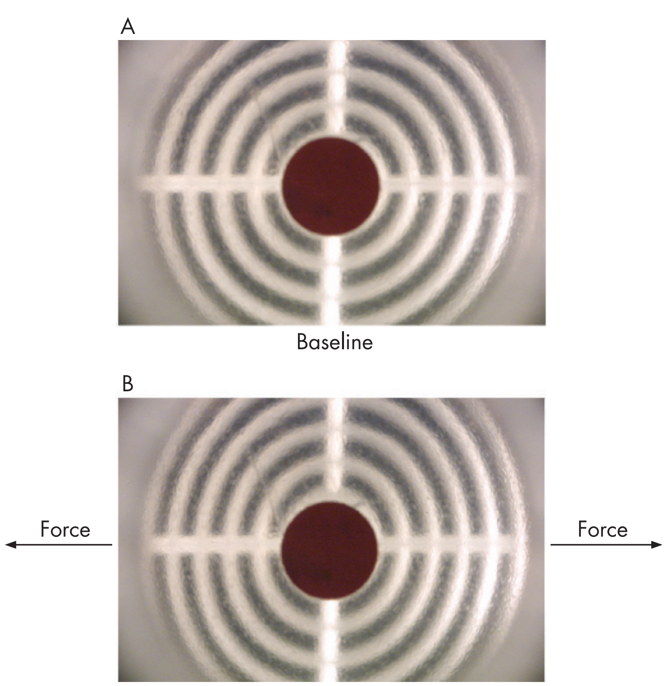

Figure 2 Reflection of the keratoscopic mires from the central surface of a water filled mylar balloon. The 6.35 mm red paper dot attached to the central surface of the balloon served as a positional reference. (A) Before equatorial traction. (B) After equatorial traction applied in the 180° meridian. Note the mires become narrower in the 180° meridian and elongated in the 90° meridian. The red paper reference dot remained the same size, stayed circular, and did not shift in the 180° meridian with equatorial traction.

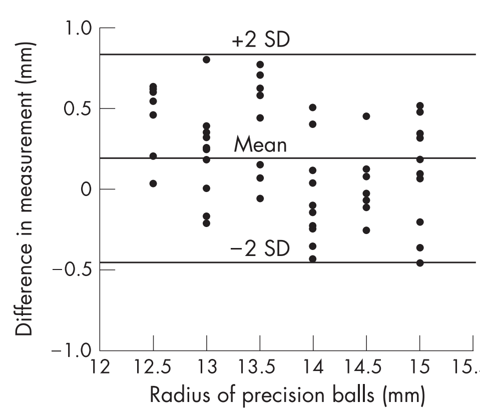

Figure 3 A Bland–Altman plot[21] of the difference between the measured radius and the actual radius of the precision balls.

Quantitative curvature change

For each 1% increase in equatorial diameter of the water filled mylar balloon, the radius of curvature decreased by 2 mm in the meridian of traction (fig 4). When equatorial traction was decreased, the radius of curvature increased in that meridian. The change in the radius of curvature in response to equatorial traction demonstrated hysteresis with full recovery to the baseline curvature (fig 4)

Vesicles

In response to an outward equatorial force, applied either externally by the laser tweezers or from within by polymerisation of the microtubular fibres, the vesicle changed shape in three distinct phases (figs 5 and 6).

First, the vesicle's profile became oval, with a decrease in central thickness and flattening of its central and peripheral surfaces. With further force, and a significant increase in its equatorial diameter, the vesicle's profile changed from oval to a *long oval*—that is, it had a minor to major axis ratio of $\leqslant 0.6$. From this second phase, only a small additional increase in force, reflected by a small increase in the vesicle's equatorial diameter, caused it to go into the third phase, where its central thickness increased, its central surfaces steepened, and its peripheral surfaces flattened (figs 5 and 6).

DISCUSSION

Positional references

Stability in shape, size, and position of the fixed reference dot relative to the camera is needed to control for any artefactual balloon movement during traction. Without this information about the stability of these reference dot parameters, changes in the mires due to movement of the balloon relative to the keratometer could be misinterpreted to reflect surface changes in the balloon.

The reference dot remained spherical in shape, unchanged in size, and stable in position in the 180° meridian during traction (fig 2). This indicates that the observed surface contour changes in the mires in the 180° meridian are real and not induced by positional balloon movements during traction.

There is evidence in the 90° meridian of a downward displacement in the positional reference dot during traction (fig 2). This downward movement, of approximately 0.5 mm, identifies tilting of the balloon during traction. This evidence of torsion in the 90° meridian confounds any interpretation of keratometric observations in the 90° meridian. Only the observations in the 180° meridian, which was stable, can be interpreted quantitatively with confidence.

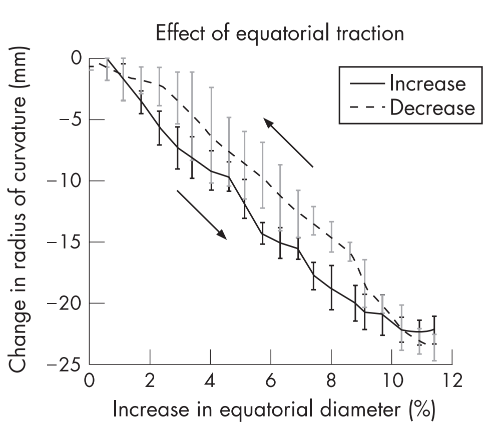

Figure 4 A graph of the mean change in the central radius of curvature of the water filled mylar balloons in the meridian of increasing (solid line) and decreasing (dashed line) equatorial traction applied in the 180° meridian. Error bars are one standard deviation of the mean.

Surface curvature change

An outward equatorial force applied to biconvex objects with a long oval profile results in central steepening and peripheral flattening. Similar shape changes occur to the profiles of air, water, and gel filled balloons and vesicles (figs 1, 2, 5, and 6). Equatorial traction was applied by astronaut Kerwin in 1973 to a freely floating 6 cubic inch drop of water in the microgravity environment of the SkyLab (NASA).[22] The central steeping and peripheral flattening of the water drop, a non-encapsulated object, are evident (fig 7).

Flattening of the central surface in response to equatorial traction only occurs when the object is initially spherical or oval. Once the object has a long oval profile,[17] similar to the profile of the human crystalline lens, additional equatorial traction inducing only a small increase in equatorial diameter results in central steepening and peripheral flattening. Whether the object has a thick or a thin capsule, a smooth capsule like the vesicles, or a capsule with wrinkles near its equator, like the balloons, these changes in shape are independent of the elastic modulus of the capsule or the compressibility of the enclosed material. These changes occurred with rubber and Mylar balloons, whether they were filled with water or gel, which is negligibly compressible, or with air, which is 15 000 times more compressible.

Human crystalline lens accommodation

Central steepening and peripheral lenticular surface flattening is associated with human in vivo accommodation and has been observed when zonular traction is applied to fresh physiologically preserved postmortem intact human lenses.[23–25] These surface changes have been demonstrated during human in vivo accommodation by each of the following: the change in position and size of reflections from the centre and peripheral anterior surface of the lens[3 4]; the change in the radius of curvature of the anterior lenticular surface with Scheimpflug photography[26] and high speed optical coherent tomography[27]; and the negative shift in spherical aberration.[1 28–30]

The lens

Capsular thickness

The lens capsule is a smooth elastic membrane and is thinner at the centre of the lens and thicker at the periphery.[4] It is, however, reasonable to simulate the lens with an object that has a capsule with uniform thickness. Mathematical modelling has demonstrated that, although the response to zonular traction is enhanced by the thickness variation of the lens capsule, the same qualitative lenticular shape changes occur if the lens capsule had uniform thickness.[31] Furthermore, it has been shown that there is no significant difference in capsular thickness between humans, primates, and rabbits even though they have significantly different accommodative amplitudes.[32]

Material properties

It is reasonable to simulate the young lens stroma with a uniform material such as water or a gel. The lens, like other biological tissues, is negligibly compressible.[33–38] In the young lens the material properties of the cortex and nucleus, including its optical density, are essentially the same.[38–40] The lens fibres are tightly packed without extracellular space.[41] The shear modulus of the young lens is very low[39] and the strength of the attachment of the lens fibres to the capsule is also very weak.[42] There is no cement substance or other extracellular material between the capsule and cortical cells. There are few interlocking processes between the first eight to 10 layers of cortical cells that are under the capsule.[41] The cortical fibres are easily hydrodissected from the lens capsule and the lens nucleus.[42–44] Consequently, the effect of interlens fibre attachments and lens

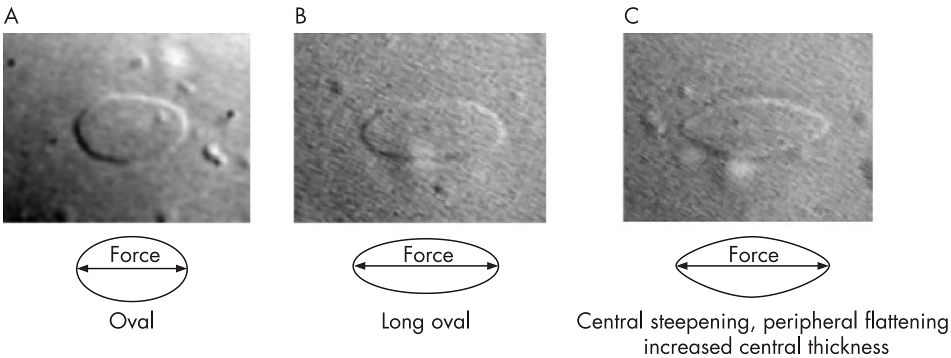

Figure 5 Vesicle profiles during an outwardly increasing equatorial force applied from within the vesicles by microtubule polymerisation. (A) Demonstrates an oval profile. (B) Demonstrates further elongation of the vesicle in the axis of force resulting in a long oval profile. (C) Demonstrates the central steepening, peripheral flattening, and increase in central thickness associated with a small increase in the equatorial diameter of the long oval profile.

sutures on the lenticular response to zonular traction is probably negligible.

Surrounding environment

The negligible compressibility of the lens results in the absence of any effect of intraocular pressure on lenticular accommodation. Experimentally, a change in intraocular pressure of up to 6 mm Hg did not alter human accommodative amplitude.[45] Consequently, the modelling of lenticular in vivo accommodation does not require that the simulating object be placed in a specialised surrounding fluid or pressure chamber.

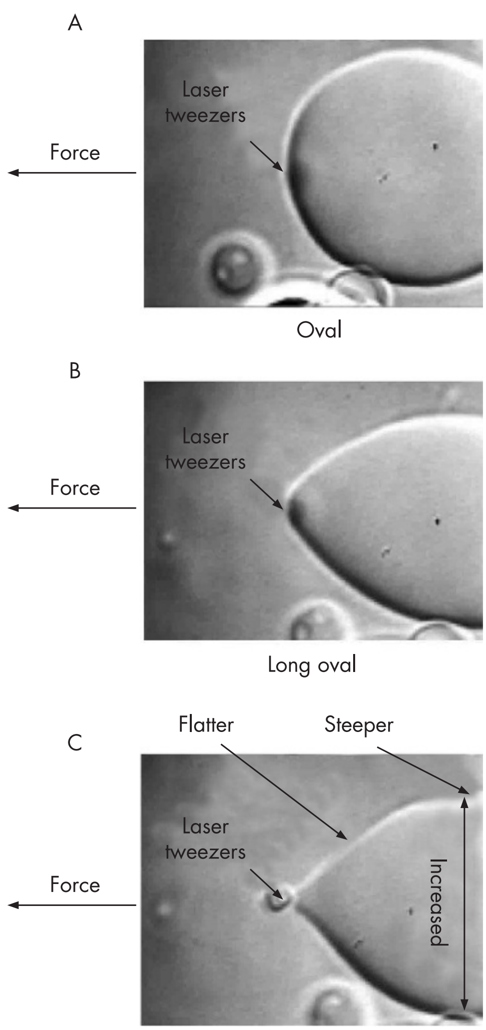

Figure 6 Vesicle profiles during application of an outwardly increasing equatorial force applied externally by optical tweezers. (A) Demonstrates an oval profile. (B) Demonstrates further elongation of the vesicle in the axis of force resulting in a long oval profile. (C) Demonstrates the central steepening, peripheral flattening, and increased central thickness associated with a small increase in the equatorial diameter of the long oval profile.

Location of tractional force

Traction was applied to the biconvex objects only at their equatorial edge. The zonules are attached anterior and posterior to the equatorial edge of the lens capsule. Finite element analysis has shown that equatorial traction applied to only the equatorial edge of the lens capsule is sufficient to simulate accommodation.[46–48]

Implications

Capsular thickness variation

In an attempt to explain the negative shift in spherical aberration that occurs during accommodation, Fincham[4]

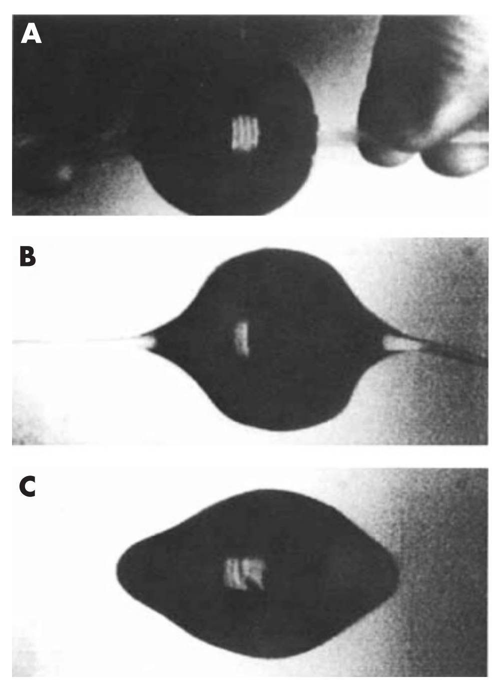

Figure 7 Changes in shape of a freely floating 6 cubic inch drop of water in the microgravity environment of the SKYLAB in response to manual application of equatorial traction. (A) Demonstrates the baseline circular water drop profile. (B) Demonstrates elongation of the water drop profile in the axis of force. (C) Demonstrates central steepening and peripheral flattening of the water drop profile (reproduced with permission from the National Aeronautics and Space Administration, NASA).

postulated that the thicker peripheral region of the lens capsule is less pliable so that as the zonules relax during accommodation the peripheral lens surface flattens as the central region of the capsule steepens. Mathematical modelling predicts the opposite,[31] and shows that during zonular relaxation the natural variation in capsular thickness enhances peripheral steepening. Our simulations also show that it is unlikely that the natural variation in capsular thickness plays a significant role in the qualitative change in lenticular shape that is associated with zonular traction. The same topographical changes occurred in response to an outward equatorial force applied to biconvex objects independent of their capsular thickness or modulus of elasticity.

Helmholtz theory

The Helmholtz theory[2] predicts that both the central and peripheral surfaces of all biconvex objects, independent of their shape, should become thinner and flatter with equatorial traction. Our simulations show that this will only occur when the biconvex object is spherical or oval.

Accommodative response

This study indicates that a small increase in equatorial diameter of objects with a long oval profile (a minor to major axis ratio of $\leqslant 0.6$) will result in central steepening and peripheral flattening of the surfaces. Human and primate lenses have a similar ratio of their central thickness to equatorial diameter after birth, always $\leqslant 0.6$.[49] Interestingly, animals that have minimal accommodative amplitude—such as mice, dogs, cats, rabbits, goats, sheep, cows, and horses—have lenses with minor axis to major axis ratios greater than 0.6.[52–56]

Conclusions

In summary, we find that an outward equatorial force applied to biconvex objects with a long oval profile, similar to the profile of the human crystalline lens, results in central steepening and peripheral surface flattening. The wide and consistent distribution of this physical change in the configuration of biconvex surfaces in response to outward equatorial force suggests the universality of these changes and why similar dynamics might be expected of the human lens during accommodation. These conclusions are opposite to those associated with the Helmholtz theory of accommodation.

Authors' affiliations

R A Schachar, Department of Physics, University of Texas at Arlington, Arlington, Texas, USA

D K Fygenson, Department of Physics, University of California, Santa Barbara, California, USA

Competing interests: Dr Schachar has a financial interest in the surgical reversal of presbyopia.

REFERENCES

1 **Young T**. On the mechanism of the eye. *Phil Trans R Soc* 1801;**92**:23–88.
2 **von Helmholtz H**. Uber die akkommodation des auges. *Arch Ophthalmol* 1844;**1**:1–74.
3 **Tscherning M**. *Physiological optics*, second edition. Philadelphia: The Keystone, 1904:160–89.
4 **Fincham EF**. Mechanism of accommodation. *Br J Ophthalmol* 1937;**8**(suppl):2–80.
5 **Weale RA**. *A biography of the eye: development, growth, age*. London: HK Lewis, 1982.
6 **Farnsworth PN**, Shyne SE. Anterior zonular shifts with age. *Exp Eye Res* 1979;**28**:291–7.
7 **Rohen JW**. Scanning electron microscopic studies of the zonular apparatus in human and monkey eyes. *Invest Ophthalmol Vis Sci* 1979;**18**:133–44.
8 **Schachar RA**. Cause and treatment of presbyopia with a method for increasing the amplitude of accommodation. *Ann Ophthalmol*, 1992;**24**:445–7,452.
9 **Tamm E**, Croft MA, Jungkunz W, *et al*. Age-related loss of ciliary muscle mobility in the rhesus monkey. Role of the choroid. *Arch Ophthalmol* 1992;**110**:871–6.
10 **Pierscionek BK**, Weale RA. Presbyopia – a maverick of human aging. *Arch Gerontol Geriatr* 1995;**20**:229–40.
11 **Schachar RA**. Is Helmholtz's theory of accommodation correct? *Ann Ophthalmol* 1999;**31**:10–17.
12 **Coleman DJ**, Fish SK. Presbyopia, accommodation, and the mature catenary. *Ophthalmology* 2001;**108**:1544–51.
13 **Strenk SA**, Strenk LM, Koretz JF. The mechanism of presbyopia. *Prog Retin Eye Res* 2005;**24**:379–93.
14 **Sarfarazi MF**. New look at the mechanism of accommodation. American Society of Cataract and Refractive Surgery, 16 April 2005, session 1-E [abstract].
15 **Schachar RA**. The mechanism of accommodation and presbyopia. *Int Ophthalmol Clin* 2006;**46**:34–61.
16 **Schachar RA**. The mechanism of accommodation and presbyopia. In:Agarwal A, editor. *Presbyopia: a surgical textbook*. Thorofare, New Jersey: Slack Inc, 2002:37–49.
17 **Rosin PL**. On Serlio's constructions of ovals. *Math Intell* 2001;**23**:58–69.
18 **Jenkins FA**, White HE. *Fundamentals of optics*, third edition. New York: McGraw-Hill, 1957:82–97.
19 **Fygenson DK**, Marko JF, Libchaber A. Mechanics of microtubule-based membrane extension. *Phys Rev Lett* 1997;**79**:4497–500.
20 **Fygenson DK**, Elbaum M, Shraiman B, Libchaber A. Microtubules and vesicles under controlled tension. *Phys Rev E* 1997;**55**:850–9.
21 **Bland JM**, Altman DG, Statistical methods for assessing agreement between two methods of clinical measurement. *Lancet*, 1986;i, 307–10.
22 **Kerwin JP**. SP-401 Skylab, classroom in space. National Aeronautics and Space Administration (NASA), 1973: http://history.nasa.gov/SP-401/p135.htm.
23 **Stadfeldt AE**. Di veränderung der lines bei traction der zonula. *Klin Monatsbl Augenheilkd* 1896;**34**:429–31.
24 **Pierscionek B**. In vitro alteration of human lens curvature by radial stretching. *Exp Eye Res*, 1993;**57**:629–35.[Central steepening secondary to zonular traction is determined by calculating the radius of curvature at x = 0 from the quadratic formulas given for the 27-year-old lens in table 1.].
25 **Schachar RA**. Qualitative effect of zonular tension on freshly extracted intact human crystalline lenses: implications for the mechanism of accommodation. *Invest Ophthalmol Vis Sci* 2004;**45**:2691–5.
26 **Dubbelman M**, Van der Heijde GL, Weeber HA. Change in shape of the aging human crystalline lens with accommodation. *Vision Res* 2005;**45**:117–32.
27 **Li Y**, Chalta MR, Huang. Measurement of lens curvature change during accommodation with high-speed optical coherence tomography. *Invest Ophthalmol Vis Sci*, 2005;**46**:E-abstract, 2554.
28 **Ninomiya S**, Fujikado T, Kuroda T, *et al*. Changes of ocular aberration with accommodation. *Am J Ophthalmol* 2002;**134**:924–6.
29 **Hazel CA**, Cox MJ, Strang NC. Wavefront aberration and its relationship to the accommodative stimulus-response function in myopic subjects. *Optom Vis Sci* 2003;**80**:151–8.
30 **Plainis S**, Ginis HS, Pallikaris A. The effect of ocular aberrations on steady-state errors of accommodative response. *J Vis* 2005;**5**:466–77.
31 **Chien CH**, Huang T, Schachar RA. Analysis of human crystalline lens accommodation. *J Biomech* 2006;**39**:672–80.
32 **Ziebarth NM**, Manns F, Uhlhorn SR, *et al*. Noncontact optical measurement of lens capsule thickness in human, monkey, and rabbit postmortem eyes. *Invest Ophthalmol Vis Sci* 2005;**46**:1690–7.
33 **Duke-Elder S**, Gloster J, Weale RA. The physiology of the eye and of vision. In:Duke-Elder S, editor.*System of ophthalmology*, vol 4.London: Henry Kimpton, 1968:365–72.
34 **Duck FA**. *Physical properties of tissue: a comprehensive reference book*. London: Academic Press, 1990:160–1.
35 **Burd HJ**, Wilde GS, Judge SJ. Can reliable values of Young's modulus be deduced from Fisher's (1971) spinning lens measurements? *Vision Res* 2006;**46**:1346–60.
36 **Subbaram MV**, Gump JC, Bullimore MA, *et al*. The elasticity of the human lens. *Invest Ophthalmol Vis Sci*, 2002;**43**:E-abstract 468..
37 **Schachar RA**. Change in intralenticular pressure during accommodation [eLetter]. *Invest Ophthal Vis Res*. 2004, http://www.iovs.org/cgi/eletters/45/2/539#169.
38 **Schachar RA**, Abolmaali A, Kamangar F. Commentary on Stachs O *et al*: Three-dimensional ultrasound, biomicroscopy environmental and conventional scanning electron microscopy investigations of the human zonula ciliaris for numerical modelling of accommodation. *Graefes Arch Clin Exp Ophthalmol* 2006;**244**:1062–3.
39 **Schachar RA**, Pierscionek BK. Lens hardness not related to the age-related decline of accommodative amplitiude. *Mol Vis* 2007;**13**:1010–1.
40 **Alio JL**, Schimchak P, Negri HP, *et al*. Crystalline lens optical dysfunction through aging. *Ophthalmology* 2005;**112**:2022–9.
41 **Hogan MJ**, Alvarado JA, Weddell JE. *Histology of the human eye*. Philadelphia: WB Saunders Co, 1971:665–73.
42 **Rakic JM**, Galand A, Vrensen GF. Separation of fibres from the capsule enhances mitotic activity of human lens epithelium. *Exp Eye Res* 1997;**64**:67–72.
43 **Ayaki M**, Ishii Y. Scanning electron microscopic observation of hydrodissected human lens nucleus. *Nippon Ganka Gakkai Zasshi* 1993;**97**:1292–7.
44 **Nordmann J**, Mack G, Mack G. Nucleus of the human lens. III. Its separation, its hardness. *Ophthalmic Res* 1974;**6**:216–22.
45 **Kurtz S**, Leibovitch I, Shemesh G, *et al*. The effect of latanoprost on accommodation in young patients with ocular hypertension. *J Glaucoma* 2003;**12**:54–6.
46 **Stachs O**, Martin H, Behrend D, *et al*. Three-dimensional ultrasound biomicroscopy, environmental and conventional scanning electron microscopy investigations of the human zonula ciliaris for numerical modelling of accommodation. *Graefes Arch Clin Exp Ophthalmol* 2006;**244**:836–44.

47 **Schachar RA**, Bax AJ. Mechanism of human accommodation as analyzed by nonlinear finite analysis. *Compr Ther* 2001;**27**:122–32.

48 **Abolmaali A**, Schachar RA, Le T. Sensitivity study of human crystalline lens accommodation. *Comput Methods Programs Biomed* 2007;**85**:77–90.

49 **Mann I**. *The development of the human eye*, third edition. New York: Grune & Stratton, 1969:46–67.

50 **Schachar RA**. Growth patterns of fresh human crystalline lenses measured by in vitro photographic biometry. *J Anat* 2005;**206**:575–80.

51 **Kuszak JR**, Peterson KL, Sivak JG, *et al*. The interrelationship of lens anatomy and optical quality. II. Primate lenses. *Exp Eye Res* 1994;**59**:521–35.

52 **Prince JH**, Diesem CD, Eglitis I, *et al*. Anatomy and histology of the eye and orbit of domestic animals. Springfield: Charles C Thomas, 1960.

53 **Pierscionek B**, Augusteyn RC. Growth related changes to functional parameters in the bovine lens. *Biochim Biophys Acta* 1992;**1116**:283–90.

54 **Sivak JG**, Herbert KL, Peterson KL, *et al*. The interrelationship of lens anatomy and optical quality. I. Non-primate lenses. *Exp Eye Res* 1994;**59**:505–20.

55 **Kuszak JR**, Zoltoski RK, Sivertson C. Fibre cell organization in crystalline lenses. *Exp Eye Res* 2004;**78**:673–87.

56 **Schachar RA**, Pierscionek BK, Abolmaali A, *et al*. The relationship between accommodative amplitude and the ratio of central lens thickness to its equational diameter in vertebrate eyes. *Br J Ophthmol* 2007;**91**:812–17.